Title

Synthesis of Carbohydrates from Methanol Using Electrochemical Partial Oxidation over Palladium with the Integrated Formose Reaction

Journal

ACS Sustainable Chemistry & Engineering, 11(34)

ISSN

2168-0485

Authors

Soland, Nathan E

Roh, Inwhan

Huynh, Wei-Shan

et al.

Publication Date

2023-08-28

DOI

10.1021/acssuschemeng.3c03426

Peer reviewed

Synthesis of carbohydrates from methanol using electrochemical partial oxidation over palladium with integrated formose reaction

Nathan E. Soland[†], Inwhan Roh[†], Wei-Shan Huynh[†], Peidong Yang[†,§,#,&]

[†]Department of Chemistry, University of California, Berkeley, California 94720, United States

[§]Department of Materials Science and Engineering, University of California, Berkeley, California 94720, United States

[#]Chemical Sciences Division, Lawrence Berkeley National Laboratory, Berkeley, California 94720, United States

[&]Kavli Energy NanoScience Institute, Berkeley, California 94720, United States

Correspondence to p_yang@berkeley.edu

Abstract

Electrochemically-derived multicarbon products are a golden target for valorization of captured carbon dioxide due to the potential of turning a waste product into useful commodity chemicals with renewable energy sources. A tantalizing approach toward their synthesis, the formose reaction utilizes homogeneous catalytic condensation of formaldehyde to generate carbohydrates. While a sustainable approach to artificial carbohydrate production through electrochemical generation of formaldehyde is desirable, to date it has not been fully realized. Here, we study the electrocatalytic conversion of methanol to formaldehyde on palladium with faradaic efficiency of over 90% at 0.9 V vs. Ag/AgCl, and with partial current density of nearly 3 mA cm^{-2} at 1.6 V vs Ag/AgCl. We observe the concurrent generation of palladium oxides as a consequence of the high overpotentials employed, which may partially explain the higher selectivity toward the partial oxidation product. Moreover, we demonstrate that formaldehyde produced electrochemically from methanol is feasible for formose reactions without need for further purification, achieving 21-28% carbon conversion to carbohydrates. This process, therefore, represents a potential avenue for electrochemical generation of formaldehyde and its utilization in generating multicarbon products inaccessible by other electrocatalytic means.

Keywords: Oxidation, formose, electrocatalysis, methanol, C_1 valorization

Introduction

A fully electrified approach to selectively yield multicarbon species from CO_2 feedstock would help enable divestment from a petrochemical economy. Direct CO_2 electroreduction efforts primarily employ copper for its unique ability to produce multicarbons such as ethylene.[1,2] However, there is limited progress in enhancing selectivity to products beyond C_2 species directly on a heterogeneous electrocatalyst due to the multitude of reaction intermediates that could be generated, their fundamental scaling relationships, and challenges associated with controlling C-C coupling on a surface.[3,4] We previously identified the electrochemically mediated formose reaction as a suitable candidate for complexification of C_1 products that may ultimately be derived from CO_2.[5] This would lead to an abiotic pathway to sugars that, if refined, could compete with plants on an energy basis.[5,6] There are two components to this approach: 1) electrochemical generation of formaldehyde (ideally from CO_2 or its derivative), and 2) its subsequent catalytically-driven conversion to carbohydrates via the formose reaction. Demonstration of the two aspects together has not yet been achieved and would present a significant advance in opening up strategies for electrocatalytic valorization of CO_2.

To address the first component of this strategy, our previous exploration of pathways for formaldehyde generation identified the partial oxidation of methanol to solution-stabilized formaldehyde as a promising route.[5] The methanol electrochemical oxidation reaction (MOR) is a widely studied reaction for its use in fuel cells.[7] As formaldehyde is a common intermediate in this pathway, the reaction may feasibly be tuned by selecting conditions favorable to partial oxidation, including catalyst selection and electrolyte conditions including electrode potential, pH, water content, and supporting electrolyte.[8–12]

The second aspect, the formose reaction, is noted for converting a concentrated solution of formaldehyde in the presence of an initiator such as glycolaldehyde and a suitable homogeneous catalyst into a complex product mixture containing carbohydrates, alcohols, and acids.[13] While the formose reaction is primarily conducted in aqueous solutions, several previous nonaqueous studies suggested that methanol could enhance yield or selectivity of the formose reaction through suppression of competing Cannizzaro reactions.[13–16] Demonstration of the reaction's robustness in the presence of methanol without interference of the supporting electrolyte from electrolysis could simplify product separation and processing for future efforts.

In this study, the effect of high anodic potential with high methanol content to generate formaldehyde is explored. These conditions allow for enhanced partial oxidation of methanol to formaldehyde, generating high concentrations suitable for employing directly into the formose reaction.

Results and Discussion

Methanol Oxidation on Palladium Foil. Palladium is noted as an active catalyst for MOR, with improved tolerance for CO generation compared to platinum alone,[17] and its higher abundance makes it an attractive candidate for manufacturing commercial MOR catalysts.[18] In alkaline MOR, deactivation of the catalyst at moderate overpotentials (around 0.8 V vs. RHE) stems from either the formation of organic poisoning species or surface (hydr)oxides which prevent methanol adsorption and inhibit deprotonation.[19–21] Therefore, its oxophilicity can lead to deactivation at potentials relevant to fuel cell operation.[22] However, reinvigoration of activity at high overpotentials, in the so-called "transpassive region,"[23] has been noted by several authors. This is possibly related to a distinct mechanism for methanol oxidation, which has not been fully described, although a recent study has noted significant formaldehyde generation on platinum.[20,24]

In this potential region, product characterization has rarely been performed, limiting insight into the reaction. The possibility to afford higher current densities and provide unique reactivity offered opportunities to investigate this potential region and its implications for formaldehyde generation.

In addition to the applied potential, solvent composition is known to play a significant role in methanol oxidation.[12] Conditions with low oxidant presence (i.e. low availability of active OH at the surface) are expected to enhance formaldehyde generation.[19] It has been reported that high faradaic efficiency to formaldehyde can be achieved with high methanol content (up to 10% water by volume).[25] On this basis, we employed 90% methanol in 10% water (v/v) for further analysis, though it is noted that we find the results are similar for a range of mixed aqueous solvent compositions with high methanol content, which can be found in the Supporting Information (Figure S1). Additionally, although palladium MOR activity may be enhanced in alkaline media,[10] high local availability of hydroxide tends to increase full oxidation to CO_2,[10,19] while strongly acidic media is less active and promotes dissolution of the catalyst.[26] To mitigate these undesired effects, we studied the neutral MOR in 0.1 M $NaClO_4$. $NaClO_4$ avoids some complicating aspects of anion adsorption to the electrode, which affects MOR activity through a selective poisoning effect.[27,28]

To better understand the behavior of the transpassive MOR, we performed bulk electrolysis at controlled potential to gain a potential-activity relationship (Figure 1a and b). Sufficient current to allow major product detection, which is limited by the lower limit of the formaldehyde assay, can only be achieved in these conditions at potentials above 0.7 V vs. Ag/AgCl (Figure 2b). At 0.9 V, faradaic efficiency (FE, a metric of selectivity) to formaldehyde is high, approaching 91 ± 9% (Figure 1a), though with low current density (11 μA cm^{-2}) (Figure 1b). As higher potentials are applied, FE decreases and current density concomitantly increases up to a maximum tested partial

current density of 2.99 mA cm^{-2} at 1.6 V (FE 58 ± 12%). Decreased current efficiency to formaldehyde at higher potential is accompanied by increased yield to CO_2 and competition with the oxygen evolution reaction (OER) (Supporting Information, Figure S2). Interestingly, these current efficiencies compare with the recent work on platinum electrodes, which in a flow cell configuration could achieve 15% FE at 25 mA cm^{-2} and 45% at 50 mA cm^{-2} on anodized platinum electrode.[24] The high current densities achieved in that work may be due to platinum being a highly active MOR catalyst combined with favorable hydrodynamics of the flow cell configuration.

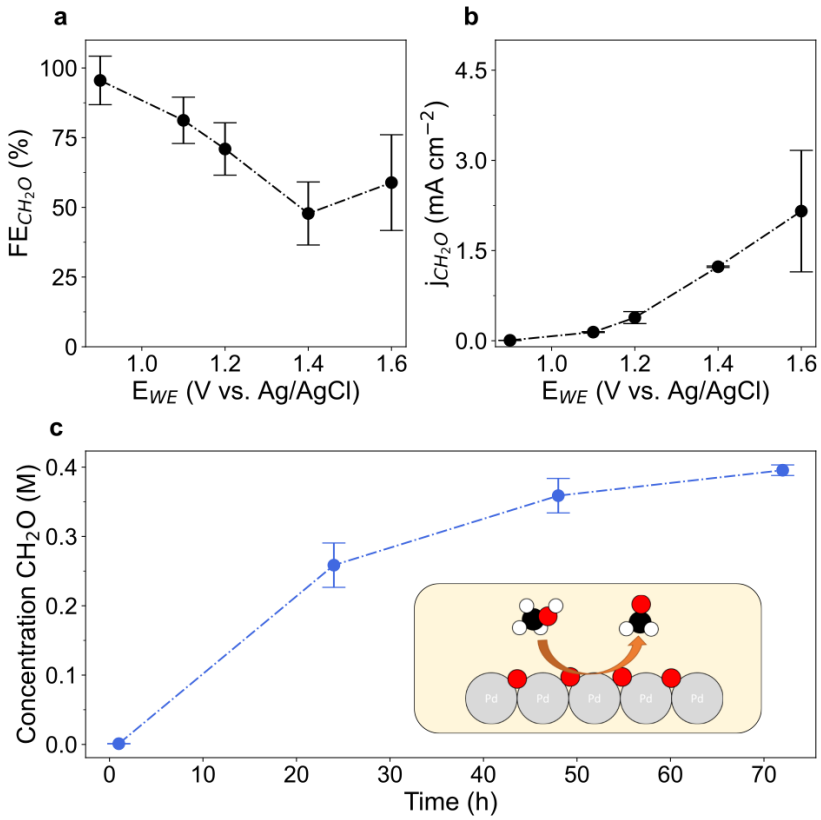

Figure 1. Electrocatalytic trials of 90% MeOH/10% H_2O (v/v). (a) Potential effect on faradaic efficiency to formaldehyde. Potential is reported as applied voltage vs. Ag/AgCl (3 M KCl). Error bars from three independent trials, each lasting one hour. (b) Partial current density toward formaldehyde from one hour potentiostatic trials. (c) Total concentration of formaldehyde in cell

as a function of time at 10 mA applied current in a galvanostatic time trial. Error bars from two independent quantification assays on a single trial. Inset: schematic illustrating the partial oxidation reaction over the palladium surface.

Galvanostatic time trial. As FE is reasonably high for all potentials studied, controlled-current conditions can be applied to reliably target high total yield of formaldehyde, a prerequisite for the formose reaction to occur. Application of 10 mA current over 72 hours allowed for generation of 0.395 M formaldehyde solution, with a cumulative FE of 49%. The apparent rate of formaldehyde accumulation decreased over time as concentrations in the cell increased, likely due to re-adsorption of formaldehyde followed by its further oxidation to CO_2 (Table S2). Additional support for this effect lies in the gradual decrease in anode potential required to maintain the current (Figure S3). This may be mitigated in conditions which increase convection at the electrode and thus remove the weakly retained formaldehyde, such as in a flow cell.

Over the course of electrolysis, the pH of the solution naturally drops due to proton abstraction,[29] with a final measured pH of 1.4. This acidification likely has a beneficial effect of stabilizing the generated formaldehyde by inhibiting the alkaline Cannizzaro reaction (where formaldehyde disproportionates to produce formic acid and methanol).[30] A secondary consideration is the possibility of electrode dissolution over time at such high potential and low pH, which may be addressed in future studies.

Presence and role of PdO_x. To understand the remarkable selectivity of the system, we aimed to evaluate the physical state of the electrode during the partial MOR. From the Pourbaix diagram, PdO_x species are expected to be thermodynamically stable at the high anodic potentials employed in this work, and thus may be the active components of the electrolysis.[31] Surface (hydr)oxides can affect adsorption behavior and deprotonation of organic species such as formaldehyde.[23]

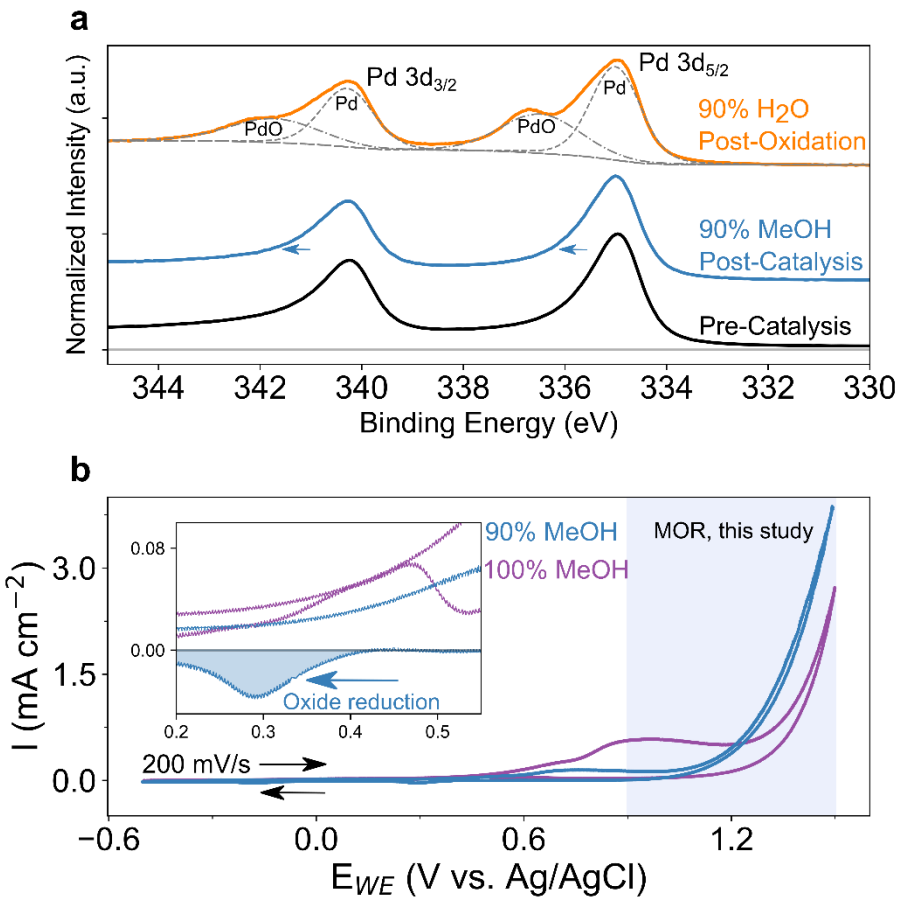

Figure 2. Evidence for the generation of oxides in the MOR and solvent effects thereon. (a) XPS spectra displaying pre- and post-catalysis surface states of palladium foil. The difference between the two spectra is minor; however, by increasing water content, it is possible to see the characteristic peak associated with the Pd oxide. (b) Steady-state cyclic voltammetry traces after repeated potential cycling (200 mV s^{-1}) of MOR on palladium foil, inset displaying a characteristic sharp reduction peak of oxide at 0.3 V vs. Ag/AgCl formed at the potentials of partial MOR.

We turned to X-ray photoelectron spectroscopy (XPS) for confirmation of oxides. The pre- and post-MOR (at 1.6 V) scans of the Pd 3d region in XPS look similar, differing primarily by increased asymmetric tailing in the post-catalysis line shapes. This may be due to enhanced

coverage of surface oxide or electronic factors that contribute to asymmetric peaks in metals.[32,33] However, with higher water content, we observed a significant amount of oxide as confirmed by the presence of a distinct Pd^{2+} $3d_{5/2}$ peak at a binding energy of 336.7 eV (Figure 2a).[34,35] Ex situ observation of a thin surface oxide is challenging due to the penetration depth of XPS exceeding that of the thin surface oxide layer combined with susceptibility of the surface oxide to reduction by the incident beam. The oxide growth be limited in the high methanol conditions of our 90% methanol v/v electrolysis as the extended growth of PdO_x requires adsorption of water.[12,36,37]

After establishing the oxides ex situ, we turned toward in situ detection with electrochemical methods, which may be more sensitive to sub-monolayer oxide films.[36] Observation of the oxides comes from cyclic voltammetry of the foil (Figure 2b). Water suppresses MOR current at lower overpotentials due to competitive adsorption. At higher anodic potentials, water may be activated and participate chemically in the oxidation of methanol, the oxidation of palladium or undergo OER over a palladium oxide film, which would reduce the faradaic efficiency of the partial MOR. In pure methanol (which contains a trace amount of water from the atmosphere), the steady-state voltammogram displays an anodic peak during the cathodic sweep at 0.5-0.6 V vs. Ag/AgCl, reminiscent of the "hysteresis" behavior of the MOR, where refreshed oxidation of methanol occurs after a small layer of oxide is removed.[20,21] With water addition, however, there is instead a cathodic peak apparent at 0.29 V, which can be attributed to dominant reduction of PdO_x species that are formed more readily from oxygen donated by water than from methanol.[23] Therefore, there are indeed surface oxide species formed during the conditions employed for the partial oxidation reaction. It is not possible on this basis to identify the specific oxide states for XPS quantitation or to decouple these from the concomitant methanol oxidation that can occur at these potentials (see Figures S4 and S5). It does, however, allow us to recognize

the interplay between methanol and water at the electrode surface and note its potential relevance to the uniquely high selectivity of the partial MOR.

As formaldehyde is repeatedly the dominant product detected, we suggest that incomplete oxidation over inert PdO_x may occur due to the lack of adjacent metallic sites required for deprotonation, a sort of site blocking effect.[12,22,38,39] Electrokinetic and spectroscopic studies on a more sensitive system, such as single crystal palladium surfaces, may help elucidate the nature of the reaction mechanism.

Methanolic formose reaction optimization. For the second component of the process, we turned our attention to the unusual aspects of the formose reaction in methanol. Before introducing the additional factor of electrolyte, we first studied the formose reaction in pure methanol using commercial paraformaldehyde (PF) as the precursor. $Ca(OH)_2$, the most widely used formose catalyst in aqueous reactions, was significantly less active in methanol than in water (Figures S6-S7). This was expected based on previous studies due to its lower solubility in methanol and possibly inhibited interaction with the hemiacetal-protected formaldehyde species.[13,14] Over the course of 120 minutes, there was no yellowing of the methanolic formose mixture, which is often considered characteristic of reaction completion.[40–42] Phenol-sulfuric assay analysis[43,44] also indicated no significant carbohydrate yield (Figure S6). However, by utilizing an alternative alkaline earth hydroxide with greater solubility, $Sr(OH)_2$, the reaction proceeded rapidly, with complete conversion as indicated by yellowing occurring within 15-20 minutes. Carbohydrate yield (formaldehyde basis) increased with more strontium catalyst, in contrast to the calcium-catalyzed aqueous reaction, which exhibits a negative relationship between carbohydrate yield and catalyst stoichiometric loading due to the fact that calcium may serve as an effective substrate for the Cannizzaro reaction in water.[41] Below a minimum formaldehyde concentration of about 0.2

M, conversion to carbohydrates was not apparent, but increasing concentration strongly enhanced the reaction, from less than 5% below 0.2 M to over 50% at 1 M (Figure S8). This set a minimum target concentration of formaldehyde of 0.2 M, which was readily exceeded in the galvanostatic time trial.

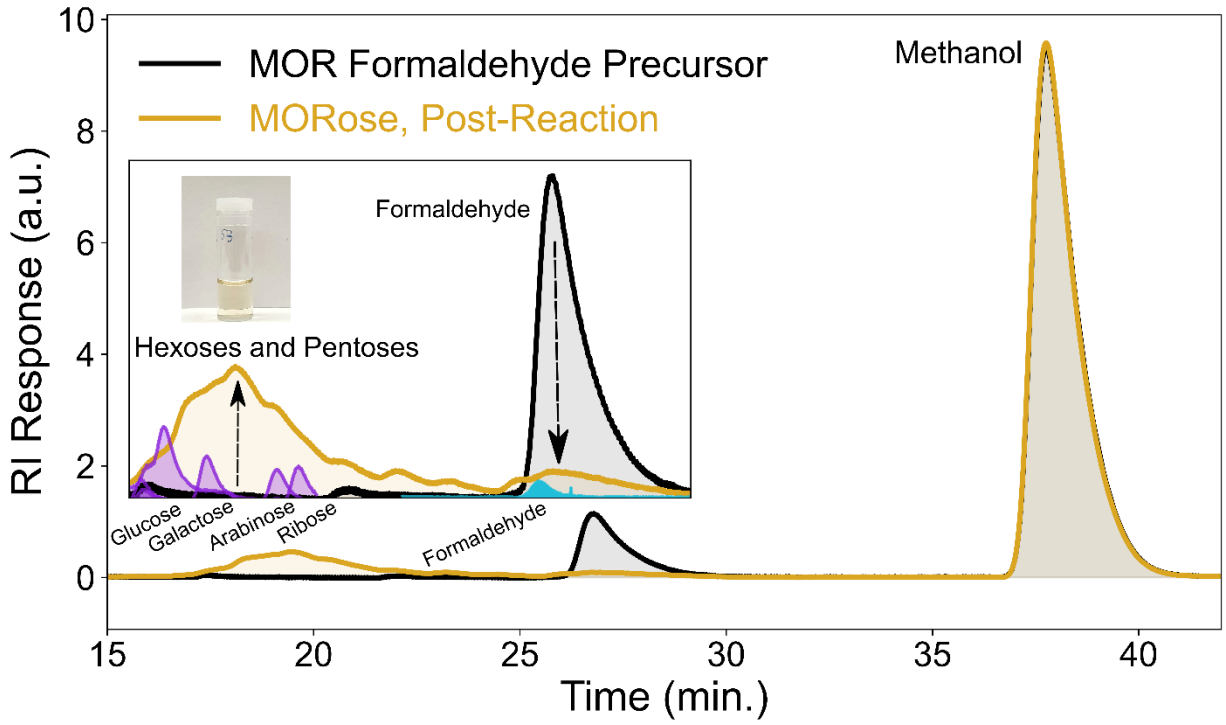

Figure 3. HPLC chromatograms of a single reaction sampled before (black) and after (yellow) the formose reaction show the consumption of formaldehyde and generation of multiple products as discrete peaks. Methanol serves as a pseudo-internal standard, confirming that formaldehyde was the major source of carbon for the reaction. Inset: expansion of the carbohydrate region of the chromatogram. Major products correspond to elution times related to C_5-C_6 species including glucose, galactose, arabinose, and ribose (standards shown in inset).

Formose from electrochemically generated formaldehyde (MORose). With the two separate aspects of the method established, we applied the optimized formose conditions to our

electrosynthesized formaldehyde solution, addressing the final question of whether supporting electrolyte and electrochemical byproducts would interfere with the formose reaction. It is well-known that formose chemistry is frequently influenced by the presence of third-party anions such as silicates and borates.[45,46] The presence of 0.1 M perchlorate in our electrolyte, however, did not inhibit the strontium-catalyzed methanolic formose reaction. The robust conversion of MOR-derived formaldehyde to sugars was established by several methods. Yellowing of the reaction occurred within 20 minutes, on a similar timescale as the PF-derived methanolic formose. We determined the yield of carbohydrates to be over 20% (24.5 ±3.5%) through the phenol-sulfuric acid assay. NMR and HPLC monitoring of samples taken during the course of reaction show the development of new products which reproduce the behavior of the aqueous formose products (Figure 3 and Figures S9-S11). Though high methanol content of solution may suppress Cannizzaro-like reactions to an extent, there was clear evidence of the development of a formate peak and some aliphatic alcohol/acids post-yellowing (Figure S10), suggesting the methanol-containing solvent is not totally sufficient for averting product loss. HPLC additionally confirms that formaldehyde was consumed during the reaction (Figure 3). Though others have noted some degree of product selectivity in the methanolic formose reaction, HPLC (Figure 3) shows a number of poorly-resolved products still result, as in the aqueous counterpart (Figure 3 and Figures S12-S13). Efficient separation of all products was not possible due to common chromatographic challenges associated with the complex mixture[47]; however, comparison of the retention times of the major products to standards of monosaccharides suggests pentoses and hexoses are formed from the reaction, in agreement with the phenol-sulfuric analysis. This data taken together supports the utility of the methanolic formose reaction for generating beyond-C_2 products from electrosynthesized formaldehyde.

Conclusion

We show that high FE can be achieved under tuned conditions on palladium foil. Exploiting neutral highly methanolic conditions decreases oxidant availability, favoring partial oxidation products. Application of high overpotential on a semi-inert oxidized palladium surface affords selectivity to formaldehyde, with increased activity at the cost of energy efficiency. This reaction is stable and was used to produce a significant concentration of formaldehyde in a methanol/water/sodium perchlorate solution, which was then directly applied in the formose reaction.

The integration of the MOR product into the formose reaction demonstrates the first deliberate generation of carbohydrates from electrochemically produced formaldehyde. $Sr(OH)_2$ allowed for significant decrease of the induction time in methanol compared to conventional $Ca(OH)_2$. This implies opportunities for further exploration of solvent conditions for integrated electro/formose chemistry.

Materials

Palladium foil (99.9%, 0.025 mm thick, Alfa Aesar) Nafion™ N-115 (0.125 mm thick, Alfa Aesar), platinum mesh and wire (99.99%) were purchased from Alfa Aesar. Methanol (Optima®, 0.2 micron filtered, Fisher Chemical), sodium perchlorate hydrate (99.99% trace metals basis), acetylacetone (puriss p.a. 99.5%, Fluka Analytical), ammonium acetate (certified A.C.S., Fisher Chemical), phenol (for molecular biology, 99%, Sigma Aldrich), sulfuric acid (certified A.C.S. plus, Fisher Chemical), perchloric acid (ACS reagent, Sigma Aldrich), D-glucose (99%, anhydrous, Thermo Scientific), formaldehyde (certified reference material, 1000 µg/mL in H_2O), strontium hydroxide (95%, Aldrich Chemistry), calcium hydroxide (95%, Sigma Aldrich) were all purchased and used without further purification. Argon (99.999% Ultra High Purity, Linde) was

used for inert conditions in electrochemical experiments. Dri-Ref, 2mm Ag/AgCl (3M KCl) reference electrode (WPI) was used for all experiments. Ultra-high purity water (18.2 MΩ-cm, TOC < 5 ppb) was generated in-house using a Millipore water purification system.

Methods

Further details of each method section may be found in the Supporting Information.

Preparation of Pd electrode. Palladium foil was sonicated in UHP water, 0.01 M $HClO_4$, and UHP water again before being electrochemically cycled in 0.01 M $HClO_4$ between -0.3 and 1 V vs. Ag/AgCl for at least 10 cycles until a reproducible CV was obtained (Figure S14). The electrode was finally rinsed with UHP water and dried under N_2 stream.

Electrochemical oxidation of methanol. A custom PEEK H-cell was employed for bulk electrolysis experiments. Potentiostatic trials were performed over one hour. 90% MeOH/10% H_2O v/v (17 mL) with 0.1 M $NaClO_4$ was the electrolyte in both chambers for the chronoamperometric experiments, while 0.1 M H_2SO_4 was employed as catholyte in the galvanostatic time trial to prevent precipitation of chloride species. Potentials are reported as applied vs Ag/AgCl due to known challenges in defining an absolute reference scale in methanol. As reference electrode construction may differ and aqueous references may be affected by methanol contamination, calibration versus ferrocenium/ferrocene is included in Figure S15.

Quantification of formaldehyde product. Formaldehyde yield was characterized using the Nash colorimetric assay. Formaldehyde concentration was obtained by comparison with a fresh calibration series generated from a formaldehyde analytical standard (Figure S16).

Formose reaction conditions. The formose reactions were carried out in this work largely as previously described.[5] Briefly, for MORose trials, the reaction was performed with the addition of

0.1 mM glycolaldehyde at 80°C with 40 mM $Sr(OH)_2$ and titration to a measured pH of 10-12 with 1M NaOH.

Quantification of sugar yield. Total C_{5+} carbohydrates were quantified using the phenol-sulfuric acid method (Figure S17).[43,44]

^{1}H-NMR of carbohydrates. A Bruker AV-600 was used to monitor the formation of carbohydrates and formose byproducts. Dimethyl sulfoxide was used as an internal standard for normalization of spectra, and the formose solution was added to D_2O in a 9:1 ratio. Solvent suppression was used to reduce the water peak.

HPLC w/ RI detection for carbohydrates. For direct confirmation of the presence of species related to C_5-C_6 products, a Dionex Ultimate 3000 HPLC equipped with an Aminex HPX-87H column was used, with an ERC RefractoMax520 RI detector. Sugar standards measured include glucose, ribose, arabinose, mannose, and fructose. Formaldehyde, methanol, and formic acid were also identified. Samples were neutralized with HCl before syringe filtration at 0.2 μM, dilution by a factor of 30 in H_2O, and direct injection into the column.

Gas product characterization. A gas chromatograph (Agilent Technologies, 7890B) was used to monitor the time-averaged formation of CO and CO_2 species during electrolysis.

Oxide identification. XPS (Thermo Scientific K-Alpha) was performed pre- and post-electrolysis to identify possible oxide states on the Pd electrode.

Author Information

Corresponding author- Peidong Yang- Department of Chemistry, University of California, Berkeley, California 94720, United States; Department of Materials Science and Engineering,

University of California, Berkeley, California 94720, United States; Kavli Energy NanoScience Institute, Berkeley, California 94720, United States.

Authors

Nathan Soland- Department of Chemistry, University of California, Berkeley, California 94720, United States.

Inwhan Roh- Department of Chemistry, University of California, Berkeley, California 94720, United States.

Wei-Shan Huynh- Department of Chemistry, University of California, Berkeley, California 94720, United States.

Associated Content

Supporting Information- Detailed experimental methods; efficiency calculations; gas products; formose optimization trials (aqueous and nonaqueous sugar yields); NMR spectra of the formose and MORose products; HPLC standards and chromatograms; assay calibrations and discussion; voltammetry.

Notes

The authors declare no competing financial interest.

Acknowledgements

This work was financially supported by the Coca-Cola Europacific Partners Ventures Program. HPLC characterization was performed using equipment belonging to the Liquid Sunlight Alliance, which is supported by the U.S. Department of Energy, Office of Science, Office of Basic Energy Sciences under award DE-SC0021266. XPS was performed at the Molecular Foundry, supported

by the Offices of Science, Office of Basic Energy Sciences, of the U.S. Department of Energy under Contract No. DE-AC02-05CH11231. The 600 MHz instrument used for characterization is from UC Berkeley's NMR facility in the College of Chemistry (CoCNMR) and supported in part by NIH S10OD024998.

References

(1) Kuhl, K. P.; Cave, E. R.; Abram, D. N.; Jaramillo, T. F. New Insights into the Electrochemical Reduction of Carbon Dioxide on Metallic Copper Surfaces. *Energy Environ. Sci.* **2012**, *5* (5), 7050–7059. https://doi.org/10.1039/C2EE21234J.
(2) Nitopi, S.; Bertheussen, E.; Scott, S. B.; Liu, X.; Engstfeld, A. K.; Horch, S.; Seger, B.; Stephens, I. E. L.; Chan, K.; Hahn, C.; Nørskov, J. K.; Jaramillo, T. F.; Chorkendorff, I. Progress and Perspectives of Electrochemical CO2 Reduction on Copper in Aqueous Electrolyte. *Chem. Rev.* **2019**, *119* (12), 7610–7672. https://doi.org/10.1021/acs.chemrev.8b00705.
(3) Peterson, A. A.; Nørskov, J. K. Activity Descriptors for CO2 Electroreduction to Methane on Transition-Metal Catalysts. *J. Phys. Chem. Lett.* **2012**, *3* (2), 251–258. https://doi.org/10.1021/jz201461p.
(4) Li, Y.; Sun, Q. Recent Advances in Breaking Scaling Relations for Effective Electrochemical Conversion of CO2. *Adv. Energy Mater.* **2016**, *6* (17), 1600463. https://doi.org/10.1002/aenm.201600463.
(5) Cestellos-Blanco, S.; Louisia, S.; Ross, M. B.; Li, Y.; Soland, N. E.; Detomasi, T. C.; Cestellos Spradlin, J. N.; Nomura, D. K.; Yang, P. Toward Abiotic Sugar Synthesis from CO2 Electrolysis. *Joule* **2022**, *6* (10), 2304–2323. https://doi.org/10.1016/j.joule.2022.08.007.
(6) Blankenship, R. E.; Tiede, D. M.; Barber, J.; Brudvig, G. W.; Fleming, G.; Ghirardi, M.; Gunner, M. R.; Junge, W.; Kramer, D. M.; Melis, A.; Moore, T. A.; Moser, C. C.; Nocera, D. G.; Nozik, A. J.; Ort, D. R.; Parson, W. W.; Prince, R. C.; Sayre, R. T. Comparing Photosynthetic and Photovoltaic Efficiencies and Recognizing the Potential for Improvement. *Science* **2011**, *332* (6031), 805–809. https://doi.org/10.1126/science.1200165.
(7) Iwasita, T. Electrocatalysis of Methanol Oxidation. *Electrochimica Acta* **2002**, *47* (22), 3663–3674. https://doi.org/10.1016/S0013-4686(02)00336-5.
(8) Hou, G.; Parrondo, J.; Ramani, V.; Prakash, J. Kinetic and Mechanistic Investigation of Methanol Oxidation on a Smooth Polycrystalline Pt Surface. *J. Electrochem. Soc.* **2013**, *161* (3), F252. https://doi.org/10.1149/2.045403jes.
(9) Rus, E. D.; Wakabayashi, R. H.; Wang, H.; Abruña, H. D. Methanol Oxidation at Platinum in Alkaline Media: A Study of the Effects of Hydroxide Concentration and of Mass Transport. *ChemPhysChem* **2021**, *22* (13), 1397–1406. https://doi.org/10.1002/cphc.202100087.
(10) Takamura, T.; Minamiyama, K. Anodic Oxidation of Methanol at Palladium Electrode in Alkaline Solution. *J. Electrochem. Soc.* **1965**, *112* (3), 333. https://doi.org/10.1149/1.2423534.

(11) Gojković, S. Lj. Mass Transfer Effect in Electrochemical Oxidation of Methanol at Platinum Electrocatalysts. *J. Electroanal. Chem.* **2004**, *573* (2), 271–276. https://doi.org/10.1016/j.jelechem.2004.07.013.
(12) Sitta, E.; Varela, H. On the Open-Circuit Interaction between Methanol and Oxidized Platinum Electrodes. *J. Solid State Electrochem.* **2008**, *12* (5), 559–567. https://doi.org/10.1007/s10008-007-0349-6.
(13) Delidovich, I. V.; Simonov, A. N.; Taran, O. P.; Parmon, V. N. Catalytic Formation of Monosaccharides: From the Formose Reaction towards Selective Synthesis. *ChemSusChem* **2014**, *7* (7), 1833–1846. https://doi.org/10.1002/cssc.201400040.
(14) Shigemasa, Y.; Taji, T.; Sakazawa, C.; Nakashima, R.; Matsuura, T. Formose Reactions: VIII. Solvent Effects in the Formose Reaction. *J. Catal.* **1979**, *58* (2), 296–302. https://doi.org/10.1016/0021-9517(79)90267-7.
(15) Shigemasa, Y.; Matsuda, Y.; Sakazawa, C.; Nakashima, R.; Matsuura, T. Formose Reactions. VI. Formose Synthesis in Methanol. *Bull. Chem. Soc. Jpn.* **1979**, *52* (4), 1091–1094. https://doi.org/10.1246/bcsj.52.1091.
(16) Shigemasa, Y.; Oogaki, K.; Ueda, N.; Hakashima, R.; Harada, K.-I.; Takeda, N.; Suzuki, M.; Saito, S. A Selective Synthesis of 3,3-Di-C-(Hydroxymethyl)-3-Deoxy-Furanorono-1,4-Lactone in the Formose Reaction. *J. Carbohydr. Chem.* **1982**, *1* (3), 325–330. https://doi.org/10.1080/07328308208085105.
(17) Chen, X.; Granda-Marulanda, L. P.; McCrum, I. T.; Koper, M. T. M. How Palladium Inhibits CO Poisoning during Electrocatalytic Formic Acid Oxidation and Carbon Dioxide Reduction. *Nat. Commun.* **2022**, *13* (1), 38. https://doi.org/10.1038/s41467-021-27793-5.
(18) Li, G.; Wang, S.; Guo, P.; Li, Y.; Zhao, X.; Li, H. Dependence of Palladium Catalysts on the Crystal Plane in the Methanol Oxidation Reaction. *J. Phys. Chem. C* **2023**, *127* (4), 1822–1827. https://doi.org/10.1021/acs.jpcc.2c07445.
(19) Mekazni, D. S.; Arán-Ais, R. M.; Ferre-Vilaplana, A.; Herrero, E. Why Methanol Electro-Oxidation on Platinum in Water Takes Place Only in the Presence of Adsorbed OH. *ACS Catal.* **2022**, *12* (3), 1965–1970. https://doi.org/10.1021/acscatal.1c05122.
(20) Chung, D. Y.; Lee, K.-J.; Sung, Y.-E. Methanol Electro-Oxidation on the Pt Surface: Revisiting the Cyclic Voltammetry Interpretation. *J. Phys. Chem. C* **2016**, *120* (17), 9028–9035. https://doi.org/10.1021/acs.jpcc.5b12303.
(21) Haisch, T.; Kubannek, F.; Nikitina, L.; Nikitin, I.; Pott, S.; Clees, T.; Krewer, U. The Origin of the Hysteresis in Cyclic Voltammetric Response of Alkaline Methanol Electrooxidation. *Phys. Chem. Chem. Phys.* **2020**, *22* (29), 16648–16654. https://doi.org/10.1039/D0CP00976H.
(22) Kakati, N.; Maiti, J.; Lee, S. H.; Jee, S. H.; Viswanathan, B.; Yoon, Y. S. Anode Catalysts for Direct Methanol Fuel Cells in Acidic Media: Do We Have Any Alternative for Pt or Pt–Ru? *Chem. Rev.* **2014**, *114* (24), 12397–12429. https://doi.org/10.1021/cr400389f.
(23) Grdeń, M.; Łukaszewski, M.; Jerkiewicz, G.; Czerwiński, A. Electrochemical Behaviour of Palladium Electrode: Oxidation, Electrodissolution and Ionic Adsorption. *Electrochimica Acta* **2008**, *53* (26), 7583–7598. https://doi.org/10.1016/j.electacta.2008.05.046.
(24) Baessler, J.; Oliveira, T.; Keller, R.; Wessling, M. Paired Electrosynthesis of Formic Acid from CO2 and Formaldehyde from Methanol. *ACS Sustain. Chem. Eng.* **2023**, *11* (18), 6822–6828. https://doi.org/10.1021/acssuschemeng.2c07523.
(25) Bélanger, G. Anodic Oxidation of Anhydrous Methanol. *J. Electrochem. Soc.* **1976**, *123* (6), 818. https://doi.org/10.1149/1.2132939.

(26) Juodkazis, K.; Juodkazytė, J.; Šebeka, B.; Stalnionis, G.; Lukinskas, A. Anodic Dissolution of Palladium in Sulfuric Acid: An Electrochemical Quartz Crystal Microbalance Study. *Russ. J. Electrochem.* **2003**, *39* (9), 954–959. https://doi.org/10.1023/A:1025724021078.
(27) Sobkowski, J.; Franaszczuk, K.; Dobrowolska, K. Effect of Anions and PH on the Adsorption and Oxidation of Methanol on a Platinum Electrode. *J. Electroanal. Chem.* **1992**, *330* (1–2), 529–540. https://doi.org/10.1016/0022-0728(92)80329-3.
(28) Romano, R. L.; Oliveira, M. G.; Varela, H. The Impact of Water Concentration on the Electro-Oxidation of Methanol on Platinum. *J. Electrochem. Soc.* **2020**, *167* (4). https://doi.org/10.1149/1945-7111/ab75c7.
(29) Iwakura, C.; Hayashi, T.; Kikkawa, S.; Tamura, H. Electrolytic Behaviour of Non-Aqueous Systems in Methanol. *Electrochimica Acta* **1972**, *17* (6), 1085–1093. https://doi.org/10.1016/0013-4686(72)90024-2.
(30) Birdja, Y. Y.; Koper, M. T. M. The Importance of Cannizzaro-Type Reactions during Electrocatalytic Reduction of Carbon Dioxide. *J. Am. Chem. Soc.* **2017**, *139* (5), 2030–2034. https://doi.org/10.1021/jacs.6b12008.
(31) POURBAIX, M. Atlas of Electrochemical Equilibria in Aqueous Solutions. *NACE* **1966**.
(32) Morgan, D. J. XPS Insights: Asymmetric Peak Shapes in XPS. *Surf. Interface Anal. n/a* (n/a). https://doi.org/10.1002/sia.7215.
(33) O'Connor, C. R.; van Spronsen, M. A.; Karatok, M.; Boscoboinik, J.; Friend, C. M.; Montemore, M. M. Predicting X-Ray Photoelectron Peak Shapes: The Effect of Electronic Structure. *J. Phys. Chem. C* **2021**, *125* (19), 10685–10692. https://doi.org/10.1021/acs.jpcc.1c01450.
(34) Peuckert, M. XPS Study on Surface and Bulk Palladium Oxide, Its Thermal Stability, and a Comparison with Other Noble Metal Oxides. *J. Phys. Chem.* **1985**, *89* (12), 2481–2486. https://doi.org/10.1021/j100258a012.
(35) Voogt, E. H.; Mens, A. J. M.; Gijzeman, O. L. J.; Geus, J. W. XPS Analysis of Palladium Oxide Layers and Particles. *Surf. Sci.* **1996**, *350* (1), 21–31. https://doi.org/10.1016/0039-6028(96)01028-X.
(36) Conway, B. E. Electrochemical Oxide Film Formation at Noble Metals as a Surface-Chemical Process. *Prog. Surf. Sci.* **1995**, *49* (4), 331–452. https://doi.org/10.1016/0079-6816(95)00040-6.
(37) Hua, Q.; Alghoraibi, N. M.; Chen, X.; Gewirth, A. A. Enhanced Methanol Oxidation Using Polymer-Incorporated Rough Pt Electrodes. *ACS Catal.* **2023**, 10683–10693. https://doi.org/10.1021/acscatal.3c01535.
(38) Li, X.; Wang, X.; Roy, K.; van Bokhoven, J. A.; Artiglia, L. Role of Water on the Structure of Palladium for Complete Oxidation of Methane. *ACS Catal.* **2020**, *10* (10), 5783–5792. https://doi.org/10.1021/acscatal.0c01069.
(39) Lustemberg, P. G.; Palomino, R. M.; Gutiérrez, R. A.; Grinter, D. C.; Vorokhta, M.; Liu, Z.; Ramírez, P. J.; Matolín, V.; Ganduglia-Pirovano, M. V.; Senanayake, S. D.; Rodriguez, J. A. Direct Conversion of Methane to Methanol on Ni-Ceria Surfaces: Metal–Support Interactions and Water-Enabled Catalytic Conversion by Site Blocking. *J. Am. Chem. Soc.* **2018**, *140* (24), 7681–7687. https://doi.org/10.1021/jacs.8b03809.
(40) Kopetzki, D.; Antonietti, M. Hydrothermal Formose Reaction. *New J. Chem.* **2011**, *35* (9), 1787–1794. https://doi.org/10.1039/C1NJ20191C.

(41) Mizuno, T.; Weiss, A. H. Synthesis and Utilization of Formose Sugars. In *Advances in Carbohydrate Chemistry and Biochemistry*; Tipson, R. S., Horton, D., Eds.; Academic Press, 1974; Vol. 29, pp 173–227. https://doi.org/10.1016/S0065-2318(08)60250-4.
(42) Omran, A.; Menor-Salvan, C.; Springsteen, G.; Pasek, M. The Messy Alkaline Formose Reaction and Its Link to Metabolism. *Life* **2020**, *10* (8), 125. https://doi.org/10.3390/life10080125.
(43) Nielsen, S. S. Phenol-Sulfuric Acid Method for Total Carbohydrates. In *Food Analysis Laboratory Manual*; Nielsen, S. S., Ed.; Food Science Texts Series; Springer US: Boston, MA, 2010; pp 47–53. https://doi.org/10.1007/978-1-4419-1463-7_6.
(44) DuBois, Michel.; Gilles, K. A.; Hamilton, J. K.; Rebers, P. A.; Smith, Fred. Colorimetric Method for Determination of Sugars and Related Substances. *Anal. Chem.* **1956**, *28* (3), 350–356. https://doi.org/10.1021/ac60111a017.
(45) Lambert, J. B.; Gurusamy-Thangavelu, S. A.; Ma, K. The Silicate-Mediated Formose Reaction: Bottom-Up Synthesis of Sugar Silicates. *Science* **2010**, *327* (5968), 984–986. https://doi.org/10.1126/science.1182669.
(46) Kim, H.-J.; Ricardo, A.; Illangkoon, H. I.; Kim, M. J.; Carrigan, M. A.; Frye, F.; Benner, S. A. Synthesis of Carbohydrates in Mineral-Guided Prebiotic Cycles. *J. Am. Chem. Soc.* **2011**, *133* (24), 9457–9468. https://doi.org/10.1021/ja201769f.
(47) Zweckmair, T.; Böhmdorfer, S.; Bogolitsyna, A.; Rosenau, T.; Potthast, A.; Novalin, S. Accurate Analysis of Formose Reaction Products by LC–UV: An Analytical Challenge. *J. Chromatogr. Sci.* **2014**, *52* (2), 169–175. https://doi.org/10.1093/chromsci/bmt004.

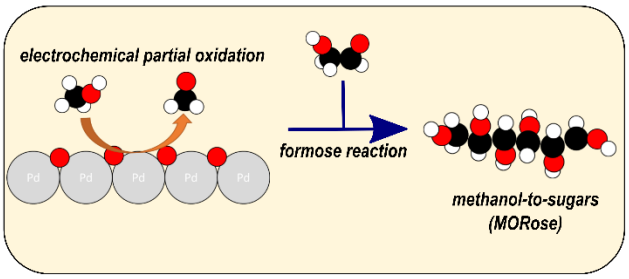

For Table of Contents Only

Synopsis: Exploiting methanol oxidation for formaldehyde generation allows for C_1 valorization without need for intermediate product purification.